Preprints of the 21st IFAC World Congress (Virtual)
Berlin, Germany, July 12-17, 2020

Implementation and Evaluation of a Sensorless, Nonlinear Stroke Controller for an Implementable, Undulating Membrane Blood Pump

**Mattias Scheffler*, Nazih Mechbal*,
Eric Monteiro*, Marc Rebillat*, Remi Pruvost****

**Laboratoire de Procedes et Ingénierie en Mecanique et Matériaux,
UMR CNRS Le CNAM, HESAM universite,151 boulevard de l'Hopital,
75013 Paris, France(e-mails : mattias.scheffler@ensam.eu, nazih.mechbal@ensam.eu,
eric.monteiro@ensam.eu, marc.rebillat@ensam.eu)*
***CorWave SA, 17 rue du Neuilly, 92110, Clichy, France (e-mail: remi.pruvost@corwave.com)*

Abstract: In this contribution, a methodology from identification to sensorless control for a vibrating membrane pump prototype is presented and evaluated, with the objective to drive an innovative cardiac assist device. For this purpose, a model of the pump is presented to design an observer-based stroke controller that only uses current measurement. Model parameters are identified experimentally with a dedicated test bench and are used to tune the controller. The control strategy is evaluated on a hydraulic test bench.

***Keywords**:* Self sensing actuators, Model identification, Biomedical mechatronics, Left ventricular assist devices.

1. INTRODUCTION

Chronic heart failure is a medical condition where the heart is unable to pump blood to sustain body needs. 2% of adults of the western hemisphere suffer from it (Savarese and Lund, 2017). It is a costly and often deadly disease. For the most severe cases, when heart transplantation is impossible, technological advances have made possible for surgeons to implant mechanical assist devices that restore blood perfusion. They consist of a pump whose inlet is connected to the left ventricle while the outlet is connected to the aorta. Blood is thus pumped directly from the left ventricle to the aorta. They are commonly named left ventricular assist device (LVAD).

Several pumping technologies have already been used for heart assistance. They are all subject to the same main requirements: the pump must be powerful enough to restore blood perfusion. The system must not be subject to failure during its operation. The pump must be small sized to be surgically implanted. The first generation was blood-filled sacs emptied by an air compressor or a pusher plate driven by an electric motor. Although capable to closely mimic the heart operation those devices lacked reliability (Yuan et al., 2012). The next generations consist of rotating pumps such as in (Griffith et al., 2001). Those are smaller, more reliable and considerably improved patient survival rates. However, those devices are sized to generate a continuous blood flow as they are operating at a near constant rotation speed. Patients using these pumps are prone to medical complication such as ventricular suction, haemolysis due to blood cell shear stress near the pump's rotating blades, or even thrombus formation and gastrointestinal bleedings. All these pumps require control laws to ensure safe operation, which is a challenge because adding sensors in the human body or in the pump itself is always detrimental in terms of biocompatibility, sizing and energy consumption.

The undulating membrane technology is originally patented in (Drevet, 2001). It is made of an inlet, an outlet and a pump body that is the space between two rigid walls where the membrane is excited at one end by a periodic force as shown in (Feier et al., 2002; Perschall et al., 2012). The excitation creates a deformation wave that propagates from the excited end to the other end that is close to the outlet. During this process, the deformation energy of the membrane is converted into kinetic energy of the fluid.

In this application of the technology (see **Figure 1**) the excitation is made by a moving magnet actuator. It is made of two coils wound inside a stator that are powered by electric current. The magnetic flux passes through a permanent magnet ring. This results in a magnetic force applied to the tip of the membrane as the magnet is fixed to it. The centring of the magnet ring around the stator is guaranteed by a set of circular springs. The operation of the pump is a challenge because unlike rotary pumps, the operation point of the undulating membrane pump is set by the amplitude and frequency of the membrane tip excitation. Indeed, the higher the stroke or frequency is, the higher the pressure head will be. It means that the stroke of the pump must be tightly controlled so it can be set fast enough to create a pressure pulse that could be synchronized with heartbeats. Care must also be given not to damage either the membrane, blood or other mechanical parts by excessive stress. Overstress can be caused by over-powering the actuator or by perturbation forces induced by the remaining activity of the heart. To simplify pump design and improve biocompatibility it is recommended to avoid adding position sensor, velocity or acceleration sensors.

Studies showing that it is possible to control moving magnet actuators without using position sensors have already been completed for similar applications. Some like (Zhang et al., 2009) compute a back electromotive force (bemf) that is proportional to velocity from an equivalent electric circuit. Estimated velocity is then integrated to get the position. It shows that it is possible to get a position estimate with an a priori knowledge of an electric model of the actuator. However, coil current derivate must be computed which makes the estimation very sensitive to measurement noise. (Latham et al., 2016) dealt with this issue by conceiving a velocity observer that does not require to compute current derivative. In those two cases, the resulting estimated position is sensitive to measurement bias in the velocity estimation that results in position drift when estimated. This effect can be bounded by adding another observer as proposed in (Aschemann et al., 2018; Mercorelli, 2017a, 2015, 2014, 2012, 2009). This second stage observers use the motion equation of the actuator and are robust to unknown force perturbations or estimate them. In all cases, these studies are limited to a domain of operation where magnetic properties of the actuator have little variations, i.e. electric parameters of the actuator are assumed to be constant. In our case, the actuator size is small compared to its performance requirements. It means that the large motion of the permanent magnet, and the high coils current will induce non-linear effects like magnetic saturation of the iron core.

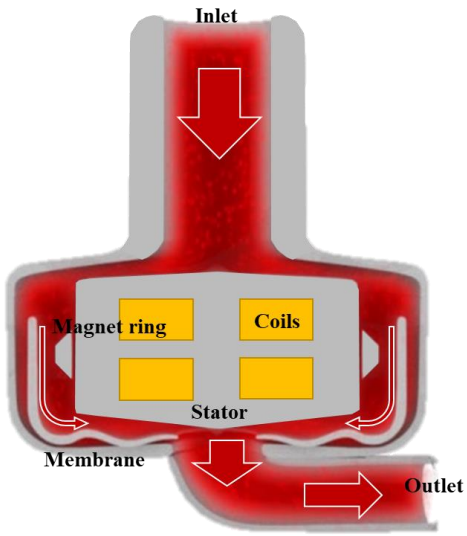

Figure 1. *Commercial schematics of the pump. Flow direction is indicated by red arrows*

Our contribution thus aims to synthetize a sensorless nonlinear stroke controller for this pump. It must be robust to pressure and flow variations of the pump, allow for a fast change of operation point and take into account magnetic non linearities. For this purpose, we propose a model of the pump that can be identified experimentally with a recursive least square algorithm, and to use that model in a control structure. We evaluate the control structure experimentally on a dedicated test bench and compare it to the case where only a linear model is used, and to the case where the observer is replaced by a position sensor.

The paper is organised as follows: Section 2 presents pump model. Section 3 details the observer-based stroke controller and the identification scheme used to calibrate the model of the real prototype. Section 4 provides results of the identification and control evaluation.

2. PUMP MODEL

The pump is composed of an electric actuator and the membrane parts, as in Figure 1. As the two coils of the actuator are connected in series, the electric circuit and the moving parts can be represented by one Kirchhoff equation and one equation of motion:

$$V_{in}(t) = RI + L(x,I)\frac{dI}{dt} + E(x,I)\frac{dx}{dt} \quad (1)$$

$$m\ddot{x}(t) = F_{mag}(x,I) + F_s(x) + F_{memb}(t) \quad (2)$$

where V_{in}, x, I, R, L and E are respectively the input voltage, magnet position, coils current, coils resistance, coils inductance and the $(bemf)$ factor E. F_{mag} represents the magnetic force generated by the actuator and F_s the spring restoring force. For this study, we assume that the membrane force F_{memb} is unknown but bounded and piecewise continuous. This assumption is motivated by the changing pressure/flow conditions during the membrane-fluid interaction that makes it complex to model $F_{memb}(t)$ by an analytic function that could be useful to the controller. The next section shows that we can develop an observer that is robust to this unmodelled force.

3. MODEL IDENTIFICATION AND SENSORLESS STROKE CONTROL

3.1. Model identification

In order to validate and adjust the above-mentioned model (1) -(2) an experimental parametric identification procedure has been performed. We have used a recursive least square estimation scheme and a proper experiment design.

Parameters R, $L(x,I)$ and $E(x,I)$ from (1) are unknown, and the variable V_{in}, I and $\frac{dI}{dt}$ are piecewise continuous. In our previous work (Scheffler et al., 2019) we proposed to estimate the 3 parameters simultaneously. Numerical experiment showed the feasibility of the method. However, from a practical viewpoint it requires some specific inputs signals to enhance the identifiability. Indeed, we need to power the coils and actuate the moving parts of the actuator independently from each other. Moreover, the persistence of excitation condition related to the convergence of the RLS algorithm specifies that the actuation frequency has to be high. Finally even if E is identified alongside R and L we would still need to measure the forces F_{mag} and F_s. We show in the following that a "static" identification coupled to a force measurement is enough to identify the whole model. Indeed, it is more efficient to assume that the motion of the actuator is negligible so $\dot{x} \simeq 0$. This means that (1) becomes:

$$V_{in}(t) = RI + L(x,I)\frac{dI}{dt} \quad (3)$$

In this case it is no more possible to estimate $E(x,I)$ alongside R and $L(x,I)$. However, a simple force sensor suffices to

measure $F_{mag}(x,I) + F_s(x)$ for all (x,I). Then it is possible to recover $E(x,I)$ with the following relation:

$$E(x,I) = \frac{\partial F_{mag}(x,I)}{\partial I} \tag{4}$$

Further information can be found about this relation in (Wiedemann, 2012). (3) can be then rewritten as:

$$y = \frac{dI}{dt} = \boldsymbol{\Psi^T \theta} \tag{5}$$

$$\boldsymbol{\theta} = \begin{bmatrix} \frac{1}{L} & \frac{R}{L} \end{bmatrix} \tag{6}$$

$$\boldsymbol{\Psi^T} = [V_{in} \quad -I] \tag{7}$$

For each sample $n > 0$, one have

$$\widehat{\boldsymbol{\theta}}_{\boldsymbol{n}} = \widehat{\boldsymbol{\theta}}_{\boldsymbol{n-1}} + \boldsymbol{K_n}(y_n - \hat{y}_n) \tag{8}$$

$$\hat{y}_n = \boldsymbol{\Psi_n^T \widehat{\theta}_{n-1}} \tag{9}$$

$$\boldsymbol{K_n} = \boldsymbol{\Psi_n Q_n} \tag{10}$$

$$\boldsymbol{Q_n} = \frac{\boldsymbol{P_{n-1}}}{\lambda + \boldsymbol{\Psi_n^T P_{n-1} \Psi_n}} \tag{11}$$

$$\boldsymbol{P_n} = \frac{1}{\lambda}\left(\boldsymbol{P_{n-1}} - \frac{\boldsymbol{P_{n-1} \Psi_n \Psi_n^T P_{n-1}}}{\lambda + \boldsymbol{\Psi_n^T P_{n-1} \Psi_n}}\right) \tag{12}$$

$0 < \lambda < 1$ is a forgetting factor, and $\boldsymbol{P_n}$ the covariance matrix. To guarantee the convergence of the algorithm we must respect the persistence of excitation condition. In a loose sense it means that all mode of the system must be excited. It can also be stated as:

$$\alpha \boldsymbol{I} \leq \sum_{n=j}^{j+S} \boldsymbol{\Psi_n^T \Psi_n} \leq \beta \boldsymbol{I} \tag{13}$$

with α, β some positive constants and S an integer.

3.2. Sensorless stroke controller

With the provided model and the means to identify it, we have to provide a controller for the pump that does not rely on a motion sensor. In the following section we will present the proposed observer-based sensorless controller. To develop the position observer, we follow a cascaded observer approach (see **Figure 2**): a first stage is devoted to the estimation the velocity of the moving parts from (1). Its output is used in a second stage, that relies on (2), which estimate the position of the moving part. This estimation is then fed back to the first stage to compute the values of $L(x,I)$ and $E(x,I)$, thus conserving the accuracy of the model used to compute velocity. Then, a controller is provided to keep the desired stroke level.

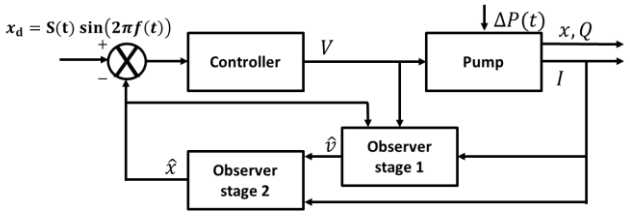

Figure 2. *pump control diagram*

3.2.1. Two stage observer

Velocity can be estimated by different approaches. The first one is to take and rewrite (1) as:

$$\hat{v} = \frac{1}{E(\hat{x},I)}\left(V_{in} - RI - L(\hat{x},I)\frac{dI}{dt}\right) \tag{14}$$

As E shows a strictly positive lower bound in the operation range of the system and I is differentiable, it is always possible to get a correct estimate of $\dot{x}$ (noted $\hat{v}$ per convention) if $\hat{x} = x$. However (14) interest is limited for a direct implementation as computing the derivative of I will be corrupted by noise. To remedy this it is possible use a low pass filter, or a derivative estimator such as in (Levant, 1998; Mboup et al., 2009). Other methods as in (Aschemann et al., 2018; Latham et al., 2016; Mercorelli, 2015, 2014) develop a dedicated observer for the velocity computation. In all cases, noise attenuation and low delay in the estimation are necessary to give a good estimate to the second stage. For practical implementation on a real time target the required sampling frequency should not be too high to not cause overflow.

For the 2nd stage, by noting $\hat{x}$ and $\hat{\dot{x}}$ are the observed position and velocity the observer is formulated as:

$$\begin{bmatrix} \hat{x} \\ \hat{\dot{x}} \end{bmatrix} = \boldsymbol{A}\begin{bmatrix} \hat{x} \\ \hat{\dot{x}} \end{bmatrix} + \begin{bmatrix} 0 \\ F(\hat{x},\hat{\dot{x}},I) \end{bmatrix} + \begin{bmatrix} k_1 \\ k_2 \end{bmatrix}\left(\hat{v} - \hat{\dot{x}}\right) \tag{15}$$

where matrix $\boldsymbol{A}$ regroup the linear part of (2), F is a function describing the non-linearities and $\boldsymbol{K} = [k_1 \quad k_2]^T$ the observer gain matrix that is chosen such that

$$\lim_{t\to\infty} \begin{bmatrix} x - \hat{x} \\ \dot{x} - \hat{\dot{x}} \end{bmatrix} = \boldsymbol{0} \tag{16}$$

(Mercorelli, 2017b) demonstrates that it is possible to choose a gain matrix that guarantee (16) and is robust to unmodelled dynamics considered as bounded, piecewise continuous perturbation forces. Nevertheless, his demonstration assumes that $\hat{v} = \dot{x}$, *i.e.*, there is no error (or negligible) in the velocity estimator. It does not guarantee the robustness regarding uncertainties acting on the measurement, which in our case would be due to an estimation error from the first stage.

3.2.2. Stroke controller

The stroke controller is designed to keep the stroke of the membrane tip close to the desired level. It consists of a feedforward and a PI controller. The feedforward is a linearization of (1) and (2) around the resting point ($x = 0, I = 0$), given in (17) and (18). It takes as input the desired position x_d at each time step to compute V_{in} as:

$$V_{in} = RI_d + L(0,0)\frac{dI_d}{t} + E(0,0)\frac{dx_d}{dt} \tag{17}$$

$$\frac{\partial F_{mag}}{\partial I}(0,0)I_d = m\ddot{x}_d - \frac{\partial F_{springs}(0)}{\partial x}x_d - \alpha\frac{dx_d}{dt} \tag{18}$$

where α represents a viscous damping coefficient that could be related to the membrane force. We choose to keep a linear formulation of the feedforward as its effect will be predominant only at start-up or at a change of operating point. The remaining unknown perturbations acting on the output are rejected by a PI controller that adjust the amplitude of the excitation. One way to estimate this amplitude is to define an amplitude estimator $\hat{S}(t)$ that is valid if $x(t)$ is sufficiently close to a sinus function, *i.e.*:

$$\hat{S}(t) = \sqrt{\hat{x}(t)^2 + \hat{x}\left(t - \frac{1}{4f(t)}\right)^2} \quad (19)$$

4. RESULTS

In this section we test the implementation of our methodology. The implementation of the identification and control algorithms is done on a DSpace MicrolabBox at a sampling frequency of 20 kHz, which is sufficiently high compared to the target frequency of our system, and sufficiently low to allow for all the required calculus to be done between each sampling. The power electronics used is an H-bridge circuit with a current sensor. Our end goal is to evaluate the whole control strategy. To validate our approach, the stroke of the pump must be set to a desired level of 0.9 mm and kept to that level for various flow conditions. In practice the minimum and maximum positions of the membrane tips must not go beyond a tolerance of $\pm 0.1mm$. If this condition is not respected, overshoots could wear out the moving parts and undershoots results in a loss of hydraulic power output. For this purpose, two dedicated test benches are used. The first one is a modified pull tester that enable the identification of the model of the pump. The second is a hydraulic circuit that to which the pump is connected. More details are available in the following sections.

4.1. Identification results

The identification test bench shown in **Figure 3**Erreur ! Source du renvoi introuvable. is composed of the pump actuator that is fixed to a strain gage who measure the springs and magnetic forces. The position of the magnet is set by an electric cylinder and measured by a laser sensor. To respect condition (13), an average current is set by a discrete PI current controller while 500 Hz frequency, 50% duty cycle square waveform is added to the voltage. The square wave amplitude is chosen to make the current signal variate around its set point with an amplitude of 0.1 A. Indeed, we find that too little excitation the of high frequency component gives us a poor estimation of the inductance. Conversely, too much current variation results in an inaccurate estimation of the inductance when saturation occurs. Sampled points are interpolated by smoothing functions and

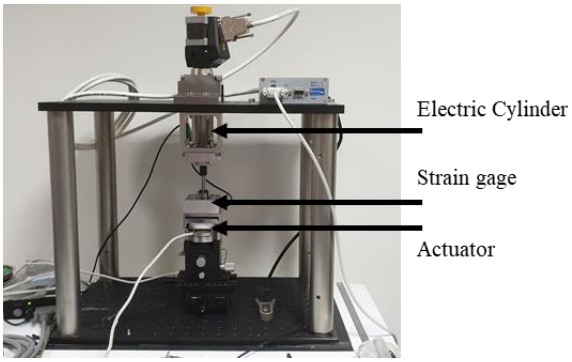

Figure 3. *Pull tester picture and schematics*

stored into lookup tables. Samples with a mean current below 0.2 A are discarded because we consider they do not respect condition (13). Results are shown in **Figure 4**Erreur ! Source du renvoi introuvable. and are in line with our expectations: measurement with an RLC meter gives an electric resistance of 3.9 **Ω**, that is close to the resistance identified, and an inductance of 22 mH, which corresponds to the value identified around the resting point of the inductance

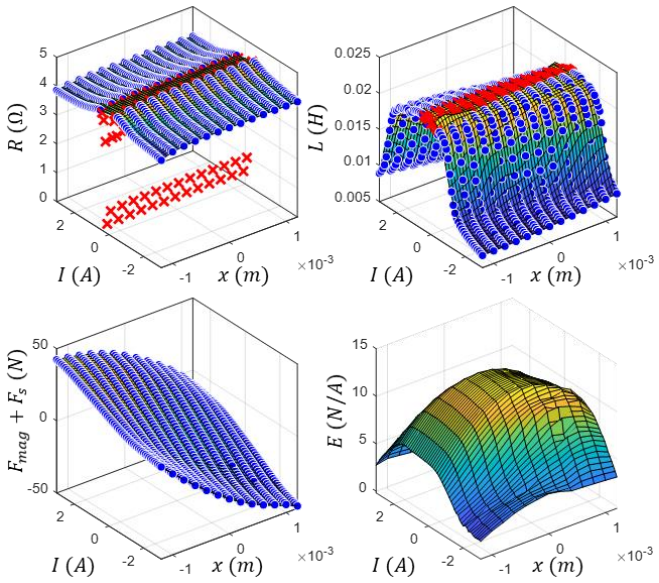

Figure 4. *Identification results. Blue dots are sampled data and red crosses are discarded samples*

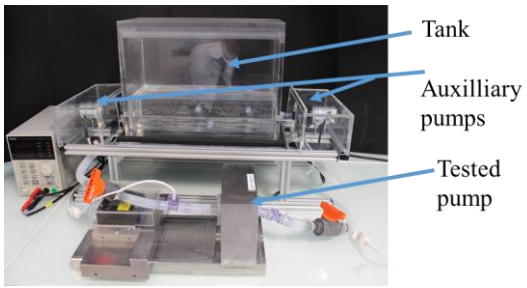

Figure 5. hydraulic test bench

4.2. Stroke control results

Once the actuator is identified, the pump is fully assembled in a transparent housing. it allows a laser measurement of the motion of the membrane tip through the housing. The pump is placed on a hydraulic test bench composed of a tank, pipes, a flow sensor and pumps that changes the flow condition of the hydraulic circuit. The fluid used during the test is a water-glycerol mixture whose viscosity is close to blood vicosity. The bench is displayed in **Figure 5**. The stroke controller is evaluated for different operation points of the pump, *i.e.*, a target stroke at various frequencies of operation and flow conditions. A result example is displayed in **Figure 6**. In this case, the frequency of actuation is set to 70 Hz, and the auxiliary pumps are turned off. Stroke reaches the desired level and is kept constant. The second test is a frequency sweep shown in Erreur ! Source du renvoi introuvable.. The controller is able to keep the desired stroke sufficiently close to its target for each frequency, where the linearized version of the observer is not. During the last test, the auxiliary pumps are turned on to lower the flow across the pump and generate a perturbation. The controller is able to keep the error below the tolerance for flow above $-6\ Lpm$ as shown in **Figure 8**

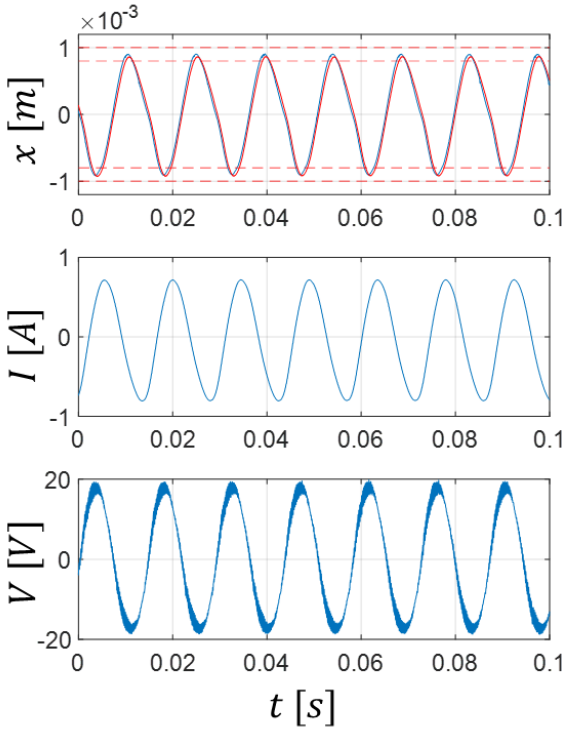

Figure 6. *Position of the moving parts, coils current and supplied voltage during pump operation. Top figure: blue is the measured position, red is the observed position. Red dashes symbolise the tolerance.*

5. DISCUSSION

This study has two objectives: the identification of a model of this actuator and its control. Regarding the identification procedure, we showed a methodology that is able to characterize almost all parts of the actuator, from coils to springs. To complete the model of the pump, two components remain to be characterized. The first is the membrane force that can only be measured or estimated during a dynamic test where the pump is immersed in a fluid and operated. The second is the effect of eddy currents in the iron core that we have neglected in the model because the actuator design is intended to minimize them. If the eddy currents were not negligible, they could affect negatively the frequency response of the stroke controller. The stroke controller is able to keep membrane stroke to the desired value for conditions that are worse than what could happen if the pump was implanted on a human patient. Indeed, in real conditions backflow is normally avoided by increasing the operation point of the pump to restore the correct flow rate. Even better, we were able to extend the operation range of the stroke controller compared to an implementation with a linear model of the actuator.

This indicates that the results presented above are encouraging. However, the convergence of the observer is not guaranteed in case there is an estimation error in the first stage. Indeed, the proof of convergence must be established in the presence of this estimation error. Based on the work of (Lien, 2004) and (Kheloufi et al., 2015), (17) is now rewritten as $y = (C + \Delta C)X$ where ΔC represents the uncertainties acting on the output due to the estimation error of the first stage. An ongoing work has led to the setting-up of convergence and stability conditions in terms of linear matrix inequalities. These results are currently experimentally tested and will be the subject of forthcoming publications.

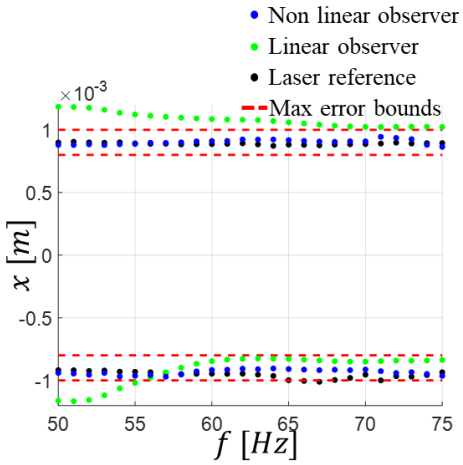

Figure 7. *Min and max position of the membrane tip during nominal operation of the pump for linear and non-linear implementation of the stroke controller. Feedback control with a laser measurement is used instead of the observer*

6. CONCLUSION

In this study we were able to formulate, implement and evaluate a stroke controller for our undulating membrane pump. The stroke is set and kept with enough accuracy for a reasonable range of operation of the pump. The addition of the non-linearities of the actuator allowed us to operate the pump beyond the validity of the linear approximation of the actuator. As discussed in Section 3.2.1 the stability of the interaction between the stages of the observer may be limited by error propagation. Convergence and stability conditions should be written down to improve the confidence of the sensorless approach.

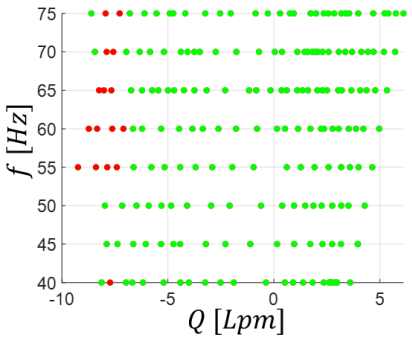

Figure 8. *Flow and frequency sweep result of the pump. Green dots indicate that the controller is able to maintain stroke while red dots indicate failure.*

7. REFERENCES

Aschemann, H., Haus, B., Mercorelli, P., 2018. Sliding Mode Control and Observer-Based Disturbance Compensation for a Permanent Magnet Linear Motor, in: 2018 Annual American Control Conference (ACC). Presented at the 2018 Annual American Control Conference (ACC),

IEEE, Milwaukee, WI, pp. 4141–4146. https://doi.org/10.23919/ACC.2018.8431787

Drevet, J.B., 2001. Vibrating membrane fluid circulator. US 2001/0001278 A1.

Feier, H., Mekkaoui, C., Drevet, J.-B., Seree, Y., Richomme, C., Rolland, P.-H., Mesana, T.G., 2002. A Novel, Valveless Ventricular Assist Device: The FishTail Pump. First Experimental In Vivo Studies. Artificial Organs 26, 1026–1031. https://doi.org/10.1046/j.1525-1594.2002.06973.x

Griffith, B.P., Kormos, R.L., Borovetz, H.S., Litwak, K., Antaki, J.F., Poirier, V.L., Butler, K.C., 2001. HeartMate II left ventricular assist system: from concept to first clinical use. The Annals of Thoracic Surgery 71, S116–S120. https://doi.org/10.1016/S0003-4975(00)02639-4

Kheloufi, H., Bedouhene, F., Zemouche, A., Alessandri, A., 2015. Observer-based stabilisation of linear systems with parameter uncertainties by using enhanced LMI conditions. International Journal of Control 88, 1189–1200. https://doi.org/10.1080/00207179.2014.999258

Latham, J., McIntyre, M.L., Mohebbi, M., 2016. Parameter Estimation and a Series of Nonlinear Observers for the System Dynamics of a Linear Vapor Compressor. IEEE Transactions on Industrial Electronics 63, 6736–6744. https://doi.org/10.1109/TIE.2016.2582728

Levant, A., 1998. Robust exact differentiation via sliding mode technique. Automatica 34, 379–384. https://doi.org/10.1016/S0005-1098(97)00209-4

Lien, C.-H., 2004. An efficient method to design robust observer-based control of uncertain linear systems. Applied Mathematics and Computation 158, 29–44. https://doi.org/10.1016/j.amc.2003.08.062

Mboup, M., Join, C., Fliess, M., 2009. Numerical differentiation with annihilators in noisy environment. Numerical Algorithms 50, 439–467. https://doi.org/10.1007/s11075-008-9236-1

Mercorelli, P., 2017a. A Motion-Sensorless Control for Intake Valves in Combustion Engines. IEEE Transactions on Industrial Electronics 64, 3402–3412. https://doi.org/10.1109/TIE.2016.2598314

Mercorelli, P., 2017b. A Motion-Sensorless Control for Intake Valves in Combustion Engines. IEEE Transactions on Industrial Electronics 64, 3402–3412. https://doi.org/10.1109/TIE.2016.2598314

Mercorelli, P., 2015. A Two-Stage Sliding-Mode High-Gain Observer to Reduce Uncertainties and Disturbances Effects for Sensorless Control in Automotive Applications. IEEE Transactions on Industrial Electronics 62, 5929–5940. https://doi.org/10.1109/TIE.2015.2450725

Mercorelli, P., 2014. An Adaptive and Optimized Switching Observer for Sensorless Control of an Electromagnetic Valve Actuator in Camless Internal Combustion Engines: An Adaptive and Optimized Switching Observer for Sensorless Control. Asian Journal of Control 16, 959–973. https://doi.org/10.1002/asjc.772

Mercorelli, P., 2012. A Two-Stage Augmented Extended Kalman Filter as an Observer for Sensorless Valve Control in Camless Internal Combustion Engines. IEEE Transactions on Industrial Electronics 59, 4236–4247. https://doi.org/10.1109/TIE.2012.2192892

Mercorelli, P., 2009. Robust feedback linearization using an adaptive PD regulator for a sensorless control of a throttle valve. Mechatronics 19, 1334–1345. https://doi.org/10.1016/j.mechatronics.2009.08.008

Perschall, M., Drevet, J.B., Schenkel, T., Oertel, H., 2012. The Progressive Wave Pump: Numerical Multiphysics Investigation of a Novel Pump Concept With Potential to Ventricular Assist Device Application: THE PROGRESSIVE WAVE PUMP. Artificial Organs 36, E179–E190. https://doi.org/10.1111/j.1525-1594.2012.01495.x

Savarese, G., Lund, L.H., 2017. Global Public Health Burden of Heart Failure. Cardiac Failure Review 3, 7–11. https://doi.org/10.15420/cfr.2016:25:2

Scheffler, M., Mechbal, N., Rebillat, M., Monteiro, E., Barabino, N., 2019. Sensorless Nonlinear Stroke Controller for an Implantable, Undulating Membrane Blood Pump, in: 58th IEEE Conference on Decision and Control. Presented at the 58th IEEE conference on decision and control, IEEE, Nice, France, p. 6.

Wiedemann, D., 2012. Permanent Magnet Reluctance Actuators for Vibration Testing. Technischen Universität München.

Yuan, N., Arnaoutakis, G.J., George, T.J., Allen, J.G., Ju, D.G., Schaffer, J.M., Russell, S.D., Shah, A.S., Conte, J.V., 2012. The Spectrum of Complications Following Left Ventricular Assist Device Placement. Journal of Cardiac Surgery 27, 630–638. https://doi.org/10.1111/j.1540-8191.2012.01504.x

Zhang, J., Chang, Y., Xing, Z., 2009. Study on Self-Sensor of Linear Moving Magnet Compressor's Piston Stroke. IEEE Sensors Journal 9, 154–158. https://doi.org/10.1109/JSEN.2008.2011098